

Whispering gallery mode resonators with J-aggregates

Dzmitry Melnikau,¹ Diana Savateeva,² Andrey Chuvilin,^{1,3} Rainer Hillenbrand^{1,3}
and Yury P. Rakovich^{2,3,*}

¹CIC nanoGune Consolider, Tolosa Hiribidea 76, Donostia-San-Sebastian, 20018, Spain

²Centro de Física de Materiales CSI-UPV/EHU, P^o Manuel de Lardizabal 5, Donostia-San Sebastian, 20018, Spain

³IKERBASQUE, Basque Foundation for Science, Alameda Urquijo 36-5, Bilbao, 48011, Spain
*yury_rakovich@ehu.es

Abstract: We have studied the optical properties of a hybrid system consisting of cyanine dye J-aggregates attached to a spherical microcavity. A periodic structure of narrow peaks was observed in the photoluminescence spectrum of the J-aggregates, arising from the coupling between the emission of J-aggregates and the whispering gallery modes (WGMs) of the microcavity. The most striking result of our study is the observation of polarization sensitive mode damping caused by re-absorption of J-aggregate emission. This effect manifests itself in dominating emission from TM modes in the spectral region of J-aggregates absorption band where the TE modes are strongly suppressed. In contrast, the TE modes totally dominate emission spectrum in the region where absorption is negligible. We also demonstrate that the emission intensity can be further enhanced by depositing a hybrid layer of J-aggregates and Ag nanoparticles onto the spherical microcavity. Owing to the concerted action of WGMs and plasmonic hot spots in the Ag aggregates, we observe an enhanced Raman signal from the J-aggregates. Microcavities covered by J-aggregates and plasmonic nanoparticles could be thus useful for a variety of photonic applications in basic science and technology.

©2011 Optical Society of America

OCIS codes: (140.4780) Optical resonators; (230.3990) Micro-optical devices; (170.4520) Optical confinement and manipulation; (240.6695) Surface-enhanced Raman scattering.

References and links

1. S. Arnold, "Microspheres, Photonic Atoms and the Physics of Nothing," *Am. Sci.* **89**, 414–421 (2001).
2. Y. P. Rakovich and J. F. Donegan, "Photonic atoms and molecules," *Laser Photonics Rev.* **4**(2), 179–191 (2010).
3. T. Kobayashi, ed., *J-Aggregates* (World Scientific, 1996).
4. N. T. Fofang, T.-H. Park, O. Neumann, N. A. Mirin, P. Nordlander, and N. J. Halas, "Plexcitonic Nanoparticles: Plasmon-Exciton Coupling in Nanoshell-J-Aggregate Complexes," *Nano Lett.* **8**(10), 3481–3487 (2008).
5. K. Yamaguchi, T. Niimi, M. Haraguchi, T. Okamoto, and M. Fukui, "Fabrication and Optical Evaluation of Silica Microsphere Coated with J-Aggregates," *Jpn. J. Appl. Phys.* **45**(8B), 6750–6753 (2006).
6. A. S. Susha, F. Caruso, A. L. Rogach, G. B. Sukhorukov, A. Kornowski, H. Möhwald, M. Giersig, A. Eychmüller, and H. Weller, "Formation of luminescent spherical core-shell particles by the consecutive adsorption of polyelectrolyte and CdTe(S) nanocrystals on latex colloids," *Colloids Surf. A* **163**(1), 39–44 (2000).
7. G. Decher and J. B. Schlenoff, *Multilayer Thin Films: Sequential Assembly of Nanocomposite Materials* (Wiley-VCH, Weinheim, 2002).
8. C. Peyratout, C. Donath, and L. Daehne, "Electrostatic interactions of cationic dyes with negatively charged polyelectrolytes in aqueous solution," *J. Photochem. Photobiol., A* **142**(1), 51–57 (2001).
9. F. C. Spano, "The Spectral Signatures of Frenkel Polarons in H- and J-Aggregates," *Acc. Chem. Res.* **43**(3), 429–439 (2010).
10. Y. Akutagawa, K. Miyasue, T. Sekiya, S. Kurita, M. Nakajima, and T. Suemoto, "Time resolved response of luminescence on cyanine dye J-aggregate," *Phys. Status Solidi C* **3**(10), 3404–3407 (2006).
11. F. C. Spano and S. Mukamel, "Superradiance in molecular aggregates," *J. Chem. Phys.* **91**(2), 683–700 (1989).
12. E. W. Knapp, "Lineshapes of molecular aggregates, exchange narrowing and intersite correlation," *Chem. Phys.* **85**, 73–82 (1984).

13. M.-L. Horng and E. L. Quitevis, "Visible Absorption Spectroscopy and Structure of Cyanine Dimers in Aqueous Solution," *J. Chem. Educ.* **77**(5), 637–639 (2000).
14. A. I. Plekhanov and V. V. Shelkovich, "Optical Constants of Nanofilms of J Aggregates of Organic dyes, Measured by Spectral Ellipsometry and Polarization Reflectometry," *Opt. Spectrosc.* **104**(4), 545–551 (2008).
15. I. Teraoka and S. Arnold, "Enhancing the sensitivity of a whispering-gallery mode microsphere sensor by a high-refractive-index surface layer," *J. Opt. Soc. Am. B* **23**(7), 1434–1441 (2006).
16. C. C. Lam, P. T. Leung, and K. Young, "Explicit asymptotic formulas for the positions, width and strength of resonances in Mie scattering," *J. Opt. Soc. Am. B* **9**(9), 1585–1592 (1992).
17. V. Chernyak, T. Meier, E. Tsiper, and S. Mukamel, "Scaling of Fluorescence Stokes Shift and Superradiance Coherence Size in Disordered Molecular Aggregates," *J. Phys. Chem. A* **103**(49), 10294–10299 (1999).
18. S. Juodkazis, K. Fujiwara, T. Takahashi, S. Matsuo, and H. Misawa, "Morphology-dependent resonant laser emission of dye-doped ellipsoidal microcavity," *J. Appl. Phys.* **91**(3), 916–921 (2002).
19. P. G. Schiro and A. S. Kwok, "Cavity-enhanced emission from a dye-coated microsphere," *Opt. Express* **12**(13), 2857–2863 (2004).
20. Y. P. Rakovich, L. Yang, E. M. McCabe, J. F. Donegan, T. Perova, A. Moore, N. Gaponik, and A. Rogach, "Whispering Gallery Mode Emission from a Composite System of CdTe Nanocrystals and a Spherical Microcavity," *Semicond. Sci. Technol.* **18**(11), 914–918 (2003).
21. S. Götzinger, L. de S. Menezes, O. Benson, D.V. Talapin, N. Gaponik, H. Weller, A.L. Rogach, V. Sandoghdar, "Confocal microscopy and spectroscopy of nanocrystals on a high-Q microsphere resonator," *J. Opt. B: Quantum Semiclassical Opt.* **6**, 154–158 (2004).
22. M. V. Artemyev and U. Woggon, "Quantum dots in photonic dots," *Appl. Phys. Lett.* **76**(11), 1353–1355 (2000).
23. S. Schietinger and O. Benson, "Coupling single NV-centres to high-Q whispering gallery modes of a preselected frequency-matched microresonator," *J. Phys. At. Mol. Opt. Phys.* **42**(11), 114001 (2009).
24. V. R. Dantham and P. B. Bisht, "Modification of radiative rates of molecules coated on a single microcavity by evanescent coupling of whispering gallery modes," *Eur. Phys. J. Appl. Phys.* **51**(2), 20902 (2010).
25. S. Holler, N. L. Goddard, and S. Arnold, "Spontaneous emission spectra from microdroplets," *J. Chem. Phys.* **108**(16), 6545–6547 (1998).
26. H. von Berlepsch, C. Bottcher, and L. Dahne, "Structure of J-Aggregates of Pseudoisocyanine Dye in Aqueous Solution," *J. Phys. Chem. B* **104**(37), 8792–8799 (2000).
27. B. Herzog, K. Huber, and H. Stegemeyer, "Aggregation of a Pseudoisocyanine Chloride in Aqueous NaCl Solution," *Langmuir* **19**(13), 5223–5232 (2003).
28. W. Kim, V. P. Safonov, V. M. Shalaev, and R. L. Armstrong, "Fractals in Microcavities: Giant Coupled, Multiplicative Enhancement of Optical Responses," *Phys. Rev. Lett.* **82**(24), 4811–4814 (1999).
29. I. M. White, J. G. Gohring, and X. Fan, "SERS-based detection in an optofluidic ring resonator platform," *Opt. Express* **15**(25), 17433–17442 (2007).
30. I. M. White, H. Oveys, and X. D. Fan, "Increasing the enhancement of SERS with dielectric microsphere resonators," *Spectroscopy* **21**, 1–5 (2006).
31. B. Trösken, F. Willig, K. Schwarzburg, A. Ehret, and M. Spitler, "The primary steps in photography: Excited J-aggregates on AgBr Microcrystals," *Adv. Mater. (Deerfield Beach Fla.)* **7**, 448–450 (1995).
32. E. C. Le Ru and P. G. Etchegoin, *Principles of Surface-Enhanced Raman Spectroscopy* (Elsevier, 2009).
33. C. Guo, M. Aydin, H.-R. Zhu, and D. L. Akins, "Density Functional Theory Used in Structure Determinations and Raman Band Assignments for Pseudoisocyanine and its Aggregate," *J. Phys. Chem. B* **106**(21), 5447–5454 (2002).
34. L. K. Ausman and G. C. Schatz, "Whispering-gallery mode resonators: Surface enhanced Raman scattering without plasmons," *J. Chem. Phys.* **129**(5), 054704 (2008).

1. Introduction

Glass or polymer microspheres also called "photonic atoms" can act as three-dimensional optical resonators providing the feedback required for the enhancement of linear and non-linear optical processes including photoluminescence (PL), bistability and Raman scattering [1]. Whispering Gallery Modes in these microcavities have been a subject of intense theoretical and experimental research paving the way for the development of single-photon emitters, nanojets, sensors and low-threshold lasers and providing the foundation for fundamental studies of optical matter interactions [2]. Nowadays the understanding gained from the studies of WGMs cavities gives the possibility of creating new materials and photonic structures with localized states in the optical spectrum. For various applications the combination of WGMs resonators with fast-emitting luminescent and/or nonlinear optical materials is especially attractive.

Among other materials, J-aggregates of organic dyes are of significant interest for the development of advanced photonic technologies thanks to their ability to delocalize and migrate excitonic energy over a large number of aggregated dye molecules. Owing to Coulomb coupling of the transition dipoles and delocalized nature of the electronic excitations, J-aggregates show the narrowest absorption and luminescence bands among

the organic materials, large value of the oscillator strength, drastic increase in spontaneous radiative emission rate with respect to monomer emission and giant third-order nonlinear susceptibility, probably the highest among both organic and inorganic materials [3]. The optical properties of J-aggregates can be further enhanced by combining them with noble-metal nanoparticles or nanoshells [4]. However, despite all these unique optical properties the integration of J-aggregates with spherical microcavities and demonstration of high-Q WGMs remained a big challenge so far [5].

In this work we developed a simple and robust method that facilitates the formation of a thin shell of J-aggregates on the surface of spherical microcavities, resulting in an efficient coupling of the J-aggregate emission with the WGMs of the microsphere. Micro-PL spectra and PL decay parameters of single microspheres covered with J-aggregates were studied. We also investigated the optical properties of microspheres covered with hybrid multi-layers consisting of J-aggregates and Ag nanoparticles.

2. Experimental details

1,1'-Diethyl-2,2'-cyanine iodide (PIC), carrying net positive charge was purchased from Sigma-Aldrich and used without further purification. Polystyrenesulfonate sodium salt (PSS), poly(allylamine hydrochloride) (PAH) and poly(diallyldimethylammonium chloride) (PDDA) were obtained from Sigma-Aldrich. MF latex microspheres of 11.93 μm in diameter were purchased from Microparticles GmbH. Colloidal silver nanoparticles (NPs) of 30 nm average size were synthesized by the conventional citrate reduction method by adding 0.8 mL of 10mM AgNO_3 to 1.4 mL of water. After adjusting the pH to 10, this solution was stirred at 0°C . Finally, 0.8 mL of 10 mM NaBH_4 was added. Doubly purified deionized water from an 18 M Ω Millipore system was used for all dilutions.

Instead of the commonly accepted chemical bonding of dye molecules to the surface of microspheres or deposition of dye-doped sol-gel film, in our experiments MF microspheres were coated with either PIC J-aggregate shell or with shell of Ag nanoparticles utilizing the layer-by-layer (LbL) assembly of the ultrathin films [6], which provides better thickness control and quality for an optoelectronic applications than films fabricated with other techniques [7].

The procedure was as follows. The particles originally possessing slightly positive surface charge were modified with monolayers of negatively charged polyelectrolyte (PSS), and positively charged polyelectrolyte (PAH or PDDA). This pretreatment allows us to increase the positive surface charge of the particles. In order to prevent direct contact of an optically active species with microsphere surface, the PSS/PAH and PSS/PDDA adsorption steps were repeated 2 times to build $\sim 3\text{nm}$ thick polyelectrolyte shell of the alternatively charged layers, finishing with a final polyelectrolyte (PE) layer of the appropriate charge (positive for deposition of the Ag NPs or negative for PIC J-aggregates). In a similar manner their combinations were also assembled on the surface of MF particles. Between all the steps of preparation, particles were carefully washed three times in water (by centrifugation) to remove the excess molecules or NPs not ionically bonded to the surface. A similar procedure was employed to deposit Ag NPs and PIC J-aggregates on the flat glass substrates by sequentially dipping a substrate into an aqueous solution of the PDDA for 20 min, followed by 20 min in the negatively charged PSS. By repeating these dipping procedures, multilayer films were assembled to the required thickness. Prior to deposition of the PE multilayer, the glass substrates were thoroughly cleaned and ultrasonicated with methanol. This rendered the substrate hydrophilic in nature and facilitated the growth of the PE layers. All sample preparation and characterization was carried out at room temperature. To prevent the bleaching of J-aggregates due to extra oxidation all spectroscopic experiments were performed on samples in aqueous solutions.

Cary 50 (Varian) and FP6600 (Jasco) were used to measure the absorption and PL spectra, respectively. Confocal Raman microscopy setup (Alpha300, WITec: 600 and 1800 mm^{-1} grating, >3 and >1 cm^{-1} spectral resolution) was used to measure micro-PL

and Raman spectra, respectively, in a backscattering geometry. A continuous wave laser emitting at 532 nm was used in the micro-PL and Raman measurements.

The time resolved PL decays were measured using a PicoQuant Microtime200 time resolved confocal microscope system, equipped with an Olympus IX71 inverted microscope. The samples were excited by picoseconds pulses generated by a PicoQuant LDH 485 laser head controlled by a Sepia II driver. The system has an overall resolution of 100 ps. PL lifetime maps that is, maps of two-dimensional in-plane variations of the PL decay times, were calculated on per pixel basis by fitting the lifetime of each pixel to the logarithm of the intensity.

Cross-sectional scanning electron microscope images (SEM) were taken using Helios NanoLab Dual Beam instrument and Environmental Scanning Electron Microscope (ESEM) Quanta 250 FEG, which was used for imaging of microspheres with wet organic shells.

3. Spherical microcavities with J-aggregates

3.1 Formation of J-aggregates triggered by PSS

In order to trigger the formation of J-aggregates we took advantage of electrostatic interaction between anionic polyelectrolyte (PSS) and cationic dye molecules of PIC with an iodide counter-ion. It was previously shown that the adsorption of PIC on PSS lead to efficient formation of J-aggregates [8]. While the monomeric PIC does not fluoresce (due to fast thermal deactivation by flip-flop motion of the two chinolyl ring system which are twisted against each other), the aggregates exhibit a narrow absorption J-band at 570 nm and strong fluorescence band with Stokes shift between them of only 3nm (Fig. 1). The PL J-band is asymmetric and exhibits a tail at longer wavelengths. The fact that the total width of the PL J-band (49 meV) exceeds the width of the J-aggregate absorption band (36 meV), is indicative of an essential manifestation of polaronic phenomenon. In case of a molecular assembly, this phenomenon involves partly distorted Franck-Condon progression and, therefore, can explain the observation of two well-resolved shoulders in PL spectra at ~616 and ~700 nm, respectively [9]. Corresponding PL decay of J-aggregates shows two-peak temporal distribution with the shortest component centered around 315 ps and the longest one grouped around 575 ps (Insert in Fig. 1b). Multiexponential PL decay is often observed in J-aggregates [10], and can be explained in terms of a distribution of exciton delocalization lengths in the sample [11].

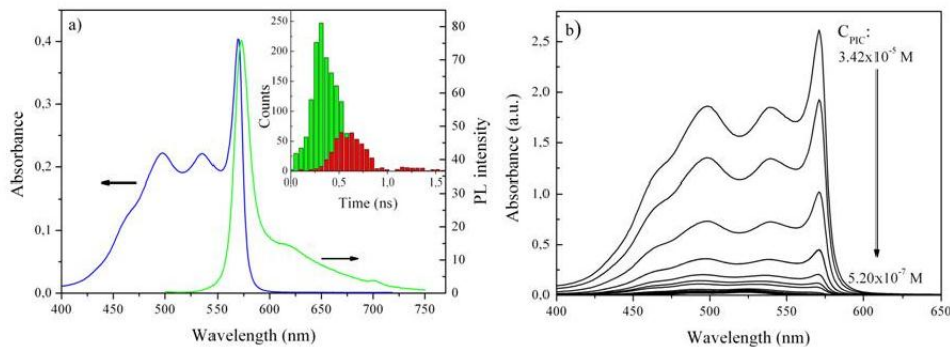


Fig. 1. a) Room-temperature absorption and PL spectra ($\lambda_{exc} = 485$ nm) of J-aggregates formed in aqueous solution of PIC by interaction with PSS. Insert: PL lifetime histogram obtained from the same sample ($\lambda_{exc} = 485$ nm, excitation power 0.05 μ W). b) Absorption spectra for serial dilutions of the J-aggregate/PSS solution.

A broad absorption band, positioned at the low-wavelength side from the J-band is related to the absorption of individual PIC molecules. It consists of the main peak centered at 535 nm and additional maximum near 498 nm followed by a shoulder at ~463 nm. It is noteworthy that the structure of the absorption spectrum of PIC monomers (including the ratio between absorbance at all maxima) is not changing much as PIC

concentration is decreased from $3.42 \times 10^{-5} \text{M}$ down to $5.2 \times 10^{-7} \text{M}$ (Fig. 1b). This allows us to assign the additional maximum and the shoulder to the vibronic transitions. Figure 1b also demonstrates high stability of formed J-aggregates under dilution conditions. Using a conventional UV-Vis spectrometer we were able to detect the J-aggregate peak at PIC concentrations as low as $2.5 \times 10^{-7} \text{M}$. At the lower concentration the absorption J-band has not been resolved due to limited sensitivity of the experimental setup.

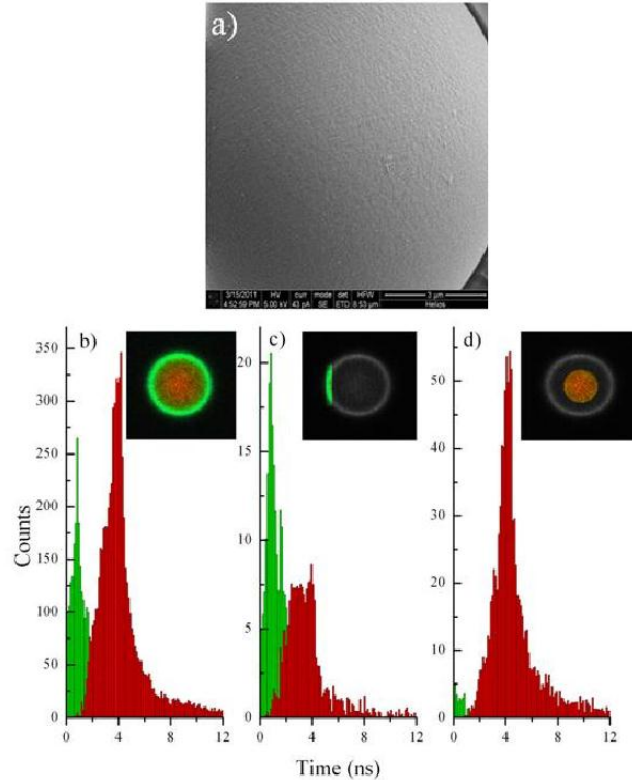


Fig. 2. SEM image of part of $11.93 \mu\text{m}$ MF microsphere with PE spacer and shell of J-aggregates (a) and PL life time histograms detected from whole microsphere (b), from the rim of the microsphere (c) and from the central part of the microsphere (d). Inserts show corresponding scanning confocal FLIM images.

Band deconvolution analysis of the absorption spectra yields 9.8 nm as full-width-at-half-maximum (fwhm) value of the J-band, whereas the corresponding value for the absorption peak of the monomer (centered at 523 nm) is 40.6 nm . These values of linewidths allow us to estimate the number of aggregated molecules across which the exciton is delocalized [12].

$$N_c = 1.5 \times (\Delta M / \Delta J)^2 \quad (1)$$

where ΔM and ΔJ are the fwhm of the absorption peaks of monomer and J-aggregate, respectively.

From the comparison of the absorption linewidths we find $N_c \sim 26$ as a lower bound for the average number of PIC molecules aggregated onto J-state. With this value and taking 1.5 nm as the length of a PIC molecule [13] we estimate the lower limit for the coherence domain (or the virtual size of the exciton delocalization) of the J-aggregates to be 39 nm . This value can also be considered as a lower limit for the physical size of the aggregates.

3.2 Integration of J-aggregates with spherical microcavity

In our experiments we aimed to take advantage of light confinement in the WGMs microcavity by placing the emitter (shell of J-aggregates) just at the rim of the microsphere, where the resonant electromagnetic field reaches its maximum. The high refractive index ($n_r = 1.68$) and optical transparency of MF make it an ideal candidate for optical applications.

The size of the MF spheres used was dictated by specific requirements for optimal excitation conditions, such as the laser wavelength matching to one of the WGMs frequencies and achieving good correlation between the WGMs and the laser linewidths. Also the wide separation of WGMs in spheres of this size allows us to avoid intricate mode mixing in the PL spectra and apply a well-known theoretical approach to the analysis of mode structure. On the other hand, the refractive index of film samples composed of PIC J-aggregates is known to be higher than 3 at the resonance [14]. It was recently shown [15] that the deposition of the layer with such a high refractive index onto the microsphere surface can tune the resonances and draw the maximal electro-magnetic field outward intensifying the evanescent field and, in our case, providing optimum conditions for efficient coupling of light emitted by J-aggregates to WGMs of the microcavity.

SEM image of the isolated microsphere, presented in Fig. 2a, demonstrates high surface quality and homogeneity of a deposited film of J-aggregates. FLIM image obtained by PL decays mapping of the whole microsphere (Fig. 2b) clearly shows the distribution of emitting species over the microsphere cross section with the dominant emission at the rim of the microcavity. Corresponding PL lifetime histogram (Fig. 2b) shows lifetime distribution that consists of two maxima centered at 0.7 and 4.2 ns. Sub-nanosecond decay is characteristic of light emitting by PIC J-aggregates (Fig. 1a). By limiting the analysis region to the rim of the microsphere (Fig. 2c) or to the central part of the microsphere (Fig. 2d) and comparing corresponding lifetime distributions we can assign the second maximum to PL detected from MF alone.

3.3 Resonant polarization sensitive WGMs damping

In contrast to the featureless PL band in the spectra of J-aggregates (Fig. 1), the emission spectrum of a single MF/J-aggregate microsphere exhibits very sharp periodic structure (Fig. 3).

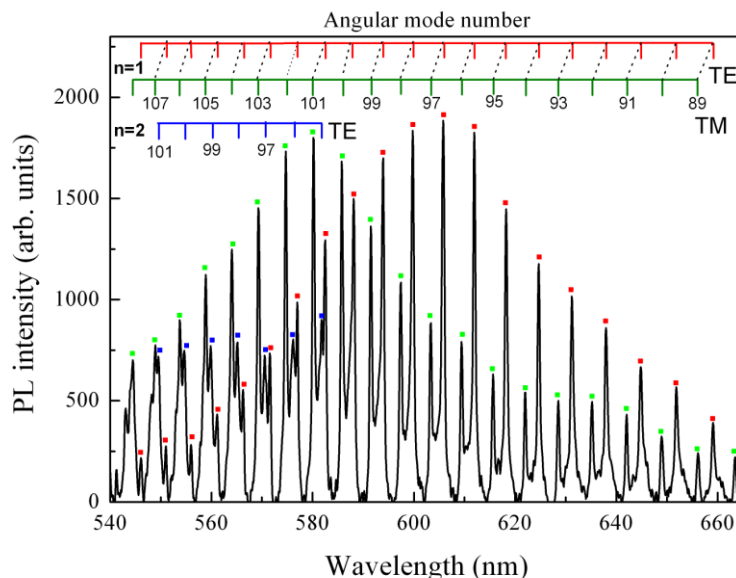


Fig. 3. Room-temperature PL spectrum from single MF microsphere covered by monolayer of J-aggregates. Inserts show the results of mode identification using Eq. (2). Green and red squares indicate TM and TE modes of first order, respectively. Blue

squares indicate TE modes of second order. As the dispersion of refractive index of MF is not known, the angular mode numbers are determined with accuracy ± 1 . The ratio between TE_{96}^1 peak intensity and background emission is 1.5.

The observed peak structure is a result of the coupling of the electronic states in J-aggregates and the photon states of the microsphere. The spectral positions and spacing between WGMs peaks are determined by the size and refractive index of a microsphere while spectral intensity distribution depends on the optical parameters of J-aggregates. Because of the high PL quantum efficiency of the J-aggregates, the WGMs in the PL spectra are superimposed on a background signal arising from the part of the J-aggregate emission, which does not match any WGMs of the microsphere. This PL background has been subtracted in the spectra presented in this paper to show the WGMs structure more clearly.

The modes in the spectrum in Fig. 3 in the spectral region above 600 nm are arranged in pairs of two pronounced peaks where the transverse electric (TE) mode corresponds to the peak with higher intensity and the transverse magnetic (TM) mode to the smaller peak. This was confirmed by polarization experiments in which the polarizer was inserted in the path of the optical beam in front of the detection system, selecting only PL signals with the component of the emitted field parallel to the polarizer. The experimentally obtained mode polarizations were verified by the calculation of spectral positions of WGMs of different polarizations using the asymptotic formula (Eq. (2) derived by Lam, Leung, and Young [16] and good agreement was obtained.

The dimensionless size parameter in Eq. (2) relates sphere radius a to the wavelength in a vacuum λ as: $x = 2\pi a/\lambda$. For a WGMs with angular mode number q and radial mode number n , the resonance size parameter is denoted as x_n^q and can be expressed as

$$n_s x_q^n = \nu + \frac{\alpha_n}{2^{1/3}} \nu^{1/3} - \frac{m p}{\sqrt{m^2 - 1}} + \frac{3\alpha_n}{10 \times 2^{2/3}} \nu^{-1/3} + \frac{m^3 p (2p^2 / 3 - 1) \alpha_n}{2^{1/3} (m^2 - 1)^{3/2}} \nu^{-2/3} + O(\nu^{-1}), \quad (2)$$

where $\nu = q + 1/2$, n_s is the refractive index of the sphere, $m = n_s/n_e$ is the relative refraction index between the sphere and the environment with refraction index n_e , $p = 1$ for TE modes, $p = 1/m^2$ for TM modes and α_n is the n -th zero of the Airy function. Comparing the results of the calculations according to the Eq. (2) with the spectral positions of the WGMs in experimental PL spectra we can identify the indices l and n . Results of this identification is shown in Fig. 3. Using the same approach we can estimate that the laser pump emission at 532 nm matches the spectral position of the TE_{111}^1 mode. This coupling is one of the conditions for the enhancement of emission of the J-aggregates deposited on the microcavity.

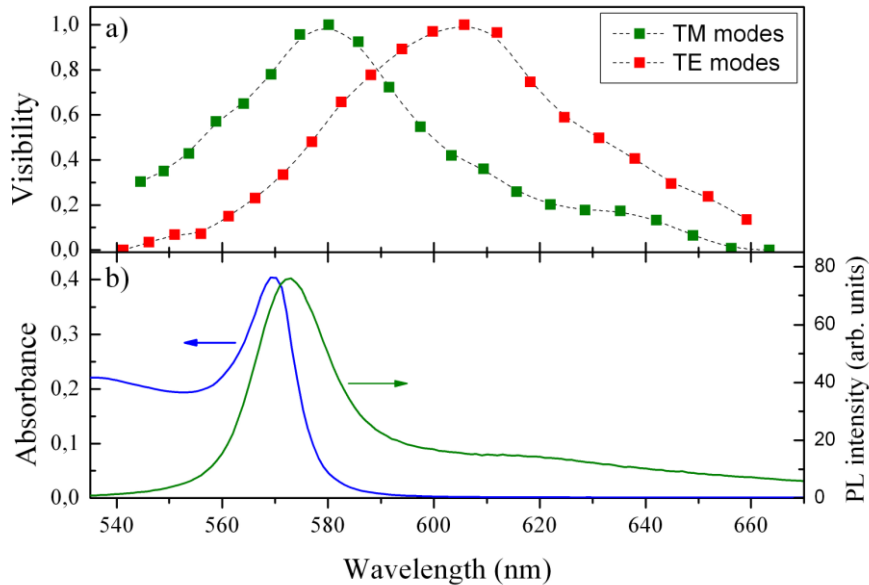


Fig. 4. a) Spectral distribution of visibility V for TM and TE mode (a) in comparison with spectral profile of absorption (blue) and PL (green) band of J-aggregates in aqueous solution. Dashed lines in (a) are a visual guide.

The Lorentzian fit of the lineshape of PL peaks allows us to estimate the values of quality factors which turned out to be ranging between 1700 and 2600 with the maximum Q value obtained for the TE_{96}^1 mode. It is noteworthy that obtained values of Q -factors are most probably strongly underestimated due to the limited spectral resolution of the experimental setup.

The procedure described above for WGMs identification allowed us to reveal another striking feature of the spectra of a single microcavity integrated with J-aggregates – different spectral distribution of maximum intensities of TE and TM WGMs (Fig. 3, Fig. 4a), defined as a mode visibility $V = (I_{\text{peak}} - I_{\text{background}}) / (I_{\text{peak}} + I_{\text{background}})$. Maximum in visibility distribution of TM modes is only slightly (by 7 nm) shifted to the red with respect to maximum of PL band of J-aggregates in aqueous solution. This shift can be explained by an increased static or a topological disorder as a result of attachment of J-aggregates to the microsphere [17]. Apart from this shift the visibility of TM modes follows reasonably well the spectral contour of PL J-band (Fig. 4a,4b). This matching provides a strong confirmation that J-aggregates are in both spectral and spatial resonance with the optical modes of a microcavity. Similar behavior have been reported for a number of other emitters attached to spherical microcavities like dye molecules [18,19], semiconductor quantum dots [20–22] or nano-diamonds containing nitrogen-vacancy centres [23]. In all these studies the distribution of TE mode visibility follows this trend too with TE modes dominating over TM modes of the same order.

A striking difference is observed for the TE modes. In our experiments, we find that the initial growth of the V value with size parameter (i.e. with decreasing wavelength) is followed by a rapid decrease in spectral region below 600 nm (Fig. 3, Fig. 4a), where absorption of J-aggregates starts rising (Fig. 4b). It thus seems that the spectral distribution of the visibility of the TE modes is shifted relative to spectral position of the PL maximum of about 25 nm. In fact, this effect is so strong, that the second-order modes dominate the TE WGMs spectrum below 590 nm (Fig. 3).

According to the theory [24], in the case of a homogeneous spherical cavity the intensity of TE modes of a given order is slightly higher than the intensity of TM modes of the same order. This is a result of the difference in spatial confinement of corresponding electro-magnetic fields with respect to the surface of a microsphere. However, it is well known that the WGMs spectra are very sensitive to the orientation and

position of the light-emitting dipole [25]. If the dipole oscillates close to the rim of the microcavity in a direction perpendicular to the microsphere surface, predominantly TM modes are excited. This is due to the fact, that only the TM modes have an electric field component in the radial direction. The dipole oscillation in the direction tangential to the microcavity surface, however, excites predominantly TE modes. Therefore TE modes will be preferentially excited by the electric field component of the attached emitter with preferential tangential orientation of transition dipole moment.

The most likely arrangement of the monomers in PIC J-aggregates is head-to-tail stacking of monomer molecules resulting in formation of fiber-like chains with a cross-sectional diameter of 2.3 nm [26] and length up to 200 nm [27] depending on the aggregation conditions. As follows from our polarization experiments combined with theoretical WGMs identification (Fig. 3), the electrostatic attachment method used in the present work produces a nanoshell of J-aggregates linked via a PE molecule spacer layer to the surface of microspheres with highly preferential tangential orientation. This alignment results in a very efficient coupling of J-aggregate emission into almost solely TE modes and in a strong increase in TE mode intensities. Moreover, the LbL deposition technique allowed us to produce layers of J-aggregates, without a stabilizing polymer and therefore to maximize the concentration of J-aggregates in a shell.

Head-to-tail aggregation of dye molecules implies that both the absorption and PL transition dipoles of the J-band are oriented along the long axis of PIC J-aggregates. Taking into account the high value of the absorption coefficient at the peak of J-band ($\alpha = 2.4 \times 10^5 \text{ cm}^{-1}$) [14] and strong overlap of the absorption and PL bands we can attribute the observed inversion from TE mode dominant emission to TM mode dominant emission in WGMs spectra to the effect of cavity enhanced re-absorption. In this process, first-generation PL photons can be efficiently confined in TE modes of the cavity and absorbed by another J-aggregates resulting in the resonant quenching of these modes. This effect is resonant with respect to the absorption band of J-aggregates and therefore is negligible in the long-wavelength spectral region where the relative strengths of TE to TM modes reflect preferentially tangential orientation of the transition moment of J-aggregates.

4. PL enhancement in a hybrid layer of J-aggregates and Ag nanoparticles

SEM images (Fig. 5) of a microsphere covered with Ag NPs and J-aggregates reveal the presence of fractal-like metallic clusters, where plasmon excitation and interaction among nanoparticles yields so called “hot spots“. These spots are nanometer-scale spatial regions of highly intense optical fields, providing a significant enhancement of Raman scattering and PL [28]. It was also suggested that very high enhancement factors can be achieved combining both electromagnetic enhancement due to surface plasmon resonances and due to the light confinement in optical microcavities [28]. This effect was demonstrated by using cylindrical microcavities filled with colloidal solution of dye and Ag NPs [28, 29], or by suspending an optical fiber with an attached microsphere into a solution of the same composition [30]. Adsorption of J-aggregates on silver or silver halide particles (such as AgBr) is of great importance in photographic science and has been studied by many groups [31].

In our experiments described below, we tested the possibility to enhance the emission of J-aggregates attached to a spherical microcavity using coupling of J-aggregate excitons to the local plasmonic fields of the metal NP clusters. To facilitate the formation of “hot spots” we used an additional procedure, which allowed us to modify the properties of the PE spacer. Before the MF spheres with PE shell were coated with a layer of Ag NPs, we kept them for 1-2 days in a NaCl solution (0.2 Mol). This treatment slightly reduces the solidity of the PE layer resulting in the formation of a more structured cross-linked shell. Formation of clusters of Ag NPs on the surface of MF sphere is clearly seen in Fig. 5.

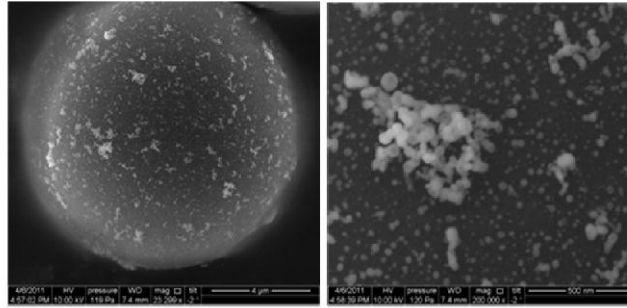


Fig. 5. SEM images of a MF microsphere with PE spacer Ag NPs.

In contrast to the microspheres with a monolayer of J-aggregates (Fig. 2a), the SEM image of the microsphere covered with Ag NPs and J-aggregates reveals the presence of rather big organic islands formed on the surface of Ag clusters (Fig. 6a). PL intensity imaging clearly demonstrates the presence of very bright spots at the rim of microspheres, which we attribute to enhanced (up to 50 times) PL from J-aggregates adsorbed on Ag clusters (Fig. 6b).

Comparison of data presented in Fig. 2b and Fig. 6d reveals another interesting phenomenon. It turned out that the PL decay lifetime of J-aggregates assembled on Ag clusters (bright spots in Fig. 6c) is 2.5 times shorter than in the case of J-aggregates attached to the MF microsphere without Ag NPs (Fig. 2b). In fact, the PL lifetime detected for J-aggregates assembled on Ag clusters (Fig. 6d) is even shorter than the PL decay time of J-aggregates in aqueous solution (Insert in Fig. 1a). The shortening of PL lifetime (along with the increase in PL intensity) is characteristic of surface-enhanced luminescence, which occurs when molecules are adsorbed on plasmon-resonant metallic nanoparticles [32]. We thus attribute the bright spots in Fig. 6b and Fig. 6c to surface-enhanced PL.

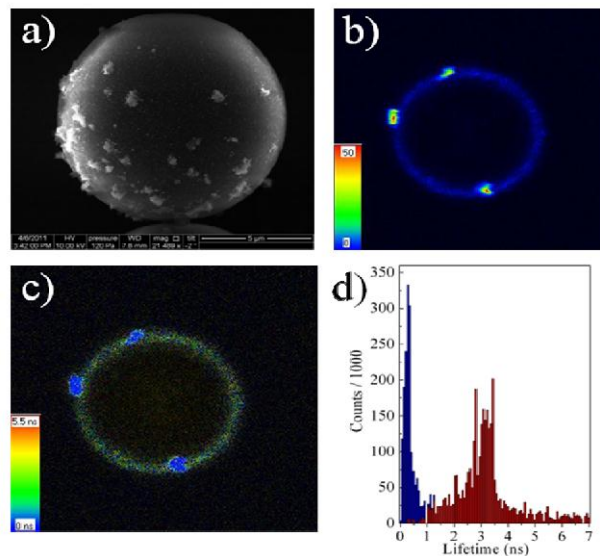


Fig. 6. Images of a MF microsphere with a PE spacer, covered with Ag NPs and a shell of J-aggregates: (a) Scanning electron microscopy image, (b) scanning confocal PL intensity image, (c) and (d) FLIM image with corresponding PL lifetime histogram.

The observed enhancement of the recombination rate is to a great extent attributed to the efficient coupling of the J-aggregate excitons to the surface plasmons of the Ag NP clusters. A large photonic mode density in the exciton-plasmon coupled system provides more radiative decay pathways. As a result, the excitons decay via plasmon interaction, which yields a shorter lifetime than the PL recombination lifetime of the J-aggregates in

the absence of the electromagnetic field due to the metal. Also the presence of Ag clusters causes dramatic changes in the PL spectra of J-aggregates attached to the surface of a microsphere. Figure 7 illustrates the substantial increase in PL intensity of the microsphere covered with Ag NPs and adsorbed J-aggregates. In the spectral region above 590 nm the PL spectrum (Fig. 7, curve 1) clearly shows a similar WGMs peak structure as observed for the microsphere without Ag NPs (Fig. 3). However, the peaks are broadened, which we assign to damping of the WGMs caused by surface plasmon excitations in the Ag NPs and scattering losses. As a result, quality factors are reduced by a factor of 6-7 relative to those obtained for the microsphere without NPs.

Along with these above mentioned WGMs, we also observe (Fig. 7, curve 1) a set of additional spectral features with four peaks distributed between 546.6 nm and 549.9 nm (group of peaks A in Fig. 7) and three most pronounced peaks centered at 569.4 nm, 573.8 nm and 582.6 nm (group B in Fig. 7). No such features were detected from a sphere without Ag NPs (Fig. 3, Fig. 7 curve 2) under the same excitation and detection conditions. To demonstrate that these peaks are the well-known Raman lines if the PIC J-aggregates, we also measured high-resolution Raman spectra (Fig. 7, curve 3) from the same microsphere and, as a control, from a glass slide with Ag NPs and J-aggregates, which does not support WGMs (Fig. 7, curve 4). Both spectra 3 and 4 exhibit the same sets of peaks as spectrum 1. Moreover, due to better spectral resolution both Raman spectra (curve 3 and 4) show the fine structure of the peaks centered at 569.4 and 573.9 nm, which is not resolved in spectrum 1. An important point is that spectral positions of all peaks in spectra 3 and 4 exactly match the positions of the Raman peaks of PIC J-aggregates reported elsewhere [33]. Three lines forming group B in these spectra are associated with the totally symmetrical in-plane deformations of individual phenyl and pyridyl rings, which are constituents of PIC molecule. These deformations give major contribution to the Raman optical activity spectra of PIC J-aggregates and therefore these Raman modes are most pronounced. Four lines which form the group A are associated with various (not necessarily totally symmetrical) deformations involving both phenyl and pyridyl rings [33].

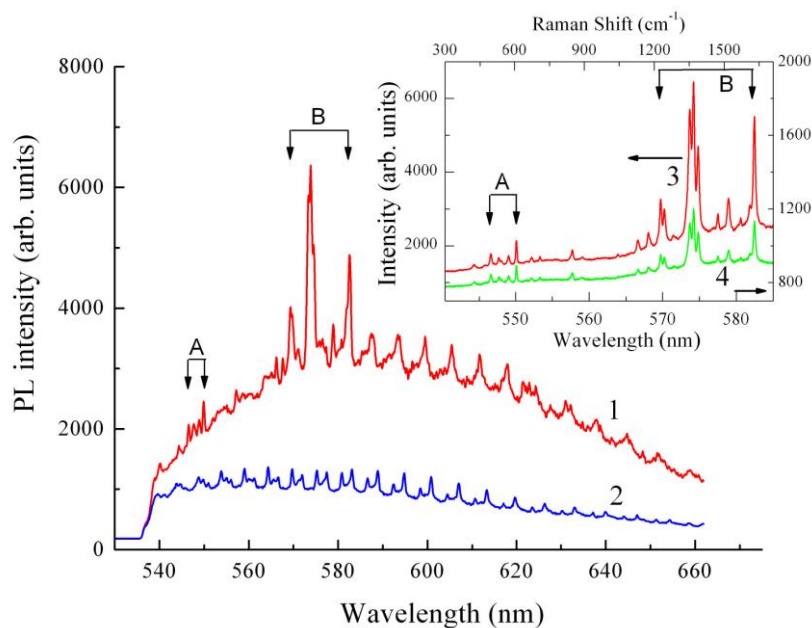


Fig. 7. Micro-PL spectra taken from a single MF microsphere covered with Ag NPs and adsorbed J-aggregates (1) and from a microsphere with shell of J-aggregates alone (2). The insert shows Raman spectra taken with higher resolution (1 cm^{-1}) from a single microsphere covered with Ag NPs and adsorbed J-aggregates (3) and from a glass slide with Ag NPs and J-aggregates (4). The Raman spectra were measured in the wavelengths that region between 540 and 585 nm. Because of the better spectral resolution one can see that

the peaks centered at 569.4 nm 573.8 nm (curve 1) consist of two and three closely spaced peaks, respectively (curves 3 and 4).

The spectra presented in Fig. 7 clearly show that in fact we have two processes working in parallel. First, the total PL of the spheres is enhanced by the Ag NPs, which can be seen by comparing the PL intensities in the WGM spectra (curves 1) with the WGM spectra of the sphere without Ag NPs. Secondly, the field enhancement provided by the Ag NPs reveals Raman lines of the J-aggregates (curve 1), which are not seen in spectrum 2. Obviously the increase of the Raman signal is stronger than the increase of the PL signals, which can be explained by the fact that the Raman intensity scales with the 4th power of the local field enhancement. Because of this well known effect [32], the Raman lines appear on the top of the enhanced PL spectrum (curve 1 in Fig. 7).

Figure 7 clearly demonstrates that the additional peaks in curve 1 of Fig. 7 (groups A and B) are Raman lines of J-aggregates adsorbed on Ag NPs. Moreover, the enhanced intensity of these Raman lines in spectrum 3 compared to the Raman lines measured on the glass slide (curve 4) indicates that the WGMs may provide an additional enhancement of the Raman signal. This assumption is supported by the fact that the peaks of group B in micro-PL spectrum (centered at 569.4 nm, 573.8 nm and 582.6 nm) perfectly match spectral positions of the TM_{103}^1 , TM_{102}^1 and TE_{101}^1 WGMs, respectively, which follows from results of a mode identification using Eq. (2). This matching is of crucial importance for the enhancement of both the PL and Raman signal as a result of complimentary effects of locally enhanced electric fields due to the WGMs resonances and localized plasmons [34].

5. Conclusions

The results presented in this work demonstrate the feasibility of the development of a high-Q optical resonator consisting of a microsphere and fast-emitting composite shell possessing a large nonlinear optical susceptibility. Many interesting possibilities can be prompted by this work. Polarization sensitive mode damping observed in the spectral region of high J-aggregate absorption can be used for suppression of unwanted modes in high Q optical whispering gallery resonators. Coupling of the plasmonic fields supported by metal nanoparticles and excitonic states of J-aggregates to microcavity local fields might be employed to manipulate the density and quality of modes and to control spontaneous emission rate in coupled hybrid system. The next step in our research on the mechanism of surface enhancement effects will be to investigate in more details the cavity assisted luminescence enhancement and enhanced Raman scattering.

Acknowledgment

The authors thank Prof. A. O. Govorov for helpful discussions.